



Project Number 101061230




DELIVERABLE D3.3

Report and prototypes of low density or hollow tungsten metal targets

Lead Beneficiary: ILL

Due date: 31/03/2024

Released on: 09/04/2024

Authors:	Ulli Köster, Stéphane Fuard	
Version:	1.1	
For the Lead Beneficiary	Reviewed by Work package Leader	Approved by Coordinator
Ulli Köster	Renata Mikołajczak	Renata Mikołajczak
	 Kierownik Projektu Prof. dr hab.inż. Renata Mikołajczak	 Kierownik Projektu Prof. dr hab.inż. Renata Mikołajczak

Dissemination Level		
PU	Public	X
RE	Restricted to a group specified by the Beneficiaries of the SECURE	
CO	Confidential, only for Beneficiaries of the SECURE project	



Funded by the
European Union

Version control table

Version number	Date of issue	Author(s)	Brief description of changes made
1.0	28.03.2024	See above	1 st draft
1.1	09.04.2024	Renata Mikolajczak Michaela Velckova	Reviewed by coordinator and MST Final version

Project information

Project number:	101061230
Project full title:	Strengthening the European Chain of supply for next generation medical Radionuclides
Acronym:	SECURE
Call and topic:	HORIZON-EURATOM-2021-NRT-01-10
Type of action:	EURATOM-RIA
Project Coordinator Organization:	NCBJ
Coordinator:	Renata Mikołajczak
EC Project Officer:	Renata Bachorczyk-Nagy
Start date – End date:	01/10/22 – 30/09/25 (36 months)
Coordinator contact:	Renata.Mikolajczak@polatom.pl
Administrative contact:	+420 245 008 599, jakub.heller@evalion.cz
Online contacts (website):	https://enen.eu/index.php/portfolio/secure-project/

Copyright

The document is proprietary of the SECURE consortium members. No copying or distributing, in any form or by any means, is allowed without the prior written agreement of the owner of the property rights. This document reflects only the authors' view. The European Commission is not liable for any use that may be made of the information contained herein.

Funded by the European Union. Views and opinions expressed are however those of the author(s) only and do not necessarily reflect those of the European Union or the European Commission. Neither the European Union nor the European Commission can be held responsible for them.

EXECUTIVE SUMMARY

Production of W-188 is performed by irradiating enriched W-186 targets in high flux reactors. Traditionally tungsten oxide targets have been used, but stability issues have occurred in the past for some of the irradiated ampoules. Thus, tungsten metal targets are sought as alternative to tungsten oxide targets.

However, large volume targets of massive tungsten are disfavoured in terms of neutronics and dissolution strategy respectively.

Notably massive and dense parts of W-186, that is a relatively strong neutron absorber, would lead to significant neutron self-attenuation in the target and consequently to a considerable reduction of yield and specific activity of the produced W-188. The neutron self-attenuation effect has been studied for different geometries by analytical estimates and Monte Carlo simulations respectively.

After irradiation the tungsten targets need to be chemically processed and the first step of this processing requires a chemical dissolution of the solid target to bring the W-188 into aqueous solution, as necessary precondition before subsequent chemical separation and/or generator loading steps. Dissolution of massive dense parts of metallic tungsten is challenging and slow since the surface-to-volume ratio is small and provides only limited liquid-solid interface area for chemical attack.

Advanced metal targets should compensate these intrinsic drawbacks of simple bulk metal targets by reducing the average physical density of the targets and/or using hollow targets to enhance their surface-to-volume ratio.

Different strategies can be followed to achieve both of these goals, namely targets of reduced physical density like foams, felts or mixtures with other materials that are weak neutron absorbers. Test samples produced by different methods have been obtained and supplied to NCBJ for dissolution tests and chemical analysis.

CONTENT

1	INTRODUCTION	5
2	NEUTRONICS ASPECTS	6
3	POSSIBLE GEOMETRIES OF ADVANCED TUNGSTEN TARGETS	12
3.1	THEORETICAL GEOMETRIES	12
3.2	FILLER MATERIALS	13
4	PRACTICAL REALISATION	14
4.1	FOAM-LIKE STRUCTURE OR ALLOY	14
4.2	WEDDING-CAKE STRUCTURE	14
4.3	PANCAKE TOWER STRUCTURE	15
4.4	HOLLOW CYLINDER	15
4.5	WIRE COIL	15
5	CONCLUSIONS AND OUTLOOK.....	16
6	ACKNOWLEDGEMENTS	17

1 INTRODUCTION

The loading of W-188/Re-188 generators requires W-188 of relatively high specific activity. W-188 is produced by double neutron capture on enriched W-186 targets that are irradiated in high flux reactors. Traditionally the targets were mainly used in form of oxide (WO_3), but tungsten metal targets are sought as alternative.

Metal targets have certain intrinsic advantages over oxide targets. Metallic tungsten has significantly, about thirtyfold, higher thermal conductivity compared to WO_3 , hence the power deposited by the nuclear heating during irradiation is dissipated more efficiently and the thermal gradient across the target and the maximum temperature in the target are considerably reduced. Moreover, the transmutation products rhenium and osmium that are generated in macroscopic quantities during long irradiations of W-186 targets do form stable alloys with tungsten and, in contrast to some of their oxides, these elements have negligible vapour pressure in elemental form and are stable at very high temperatures (e.g. used as thermocouples). Altogether, these facts will effectively prevent the thermochemical stability issues that have been observed during past irradiations of tungsten oxide targets (cf. deliverable D3.1).

However, large volume targets of dense tungsten metal are disfavoured in terms of neutronics and dissolution strategy respectively.

Notably massive and dense parts of W-186, that is a relatively strong neutron absorber, would lead to significant neutron self-shielding in the target and consequently to a considerable reduction of yield and specific activity of the produced W-188.

The irradiated tungsten targets need to be chemically processed after irradiation and the first step of this processing requires a chemical dissolution of the solid target to bring the W-188 into aqueous solution, as necessary precondition before subsequent chemical separation and/or generator loading steps. Dissolution of massive dense parts of metallic tungsten is challenging and slow since the surface-to-volume ratio is small and provides only limited liquid-solid interface area for chemical attack.

Advanced metal targets should compensate these intrinsic drawbacks of simple bulk metal targets by reducing the average physical density of the targets and by enhancing their surface-to-volume ratio.

Different strategies can be followed to achieve these goals and are discussed in the following, together with preparation of test samples by different methods.

2 NEUTRONICS ASPECTS

The generation of W-188 requires two subsequent neutron captures on W-186 targets: $W-186(n,\gamma)W-187(n,\gamma)W-188$, see Figure 1. This specific reaction path is peculiar for W-188 and distinct from the production of most other radionuclides, that are mostly based on a single reaction step (that may be induced by neutrons, photons or charged particles respectively), sometimes combined with the radioactive decay of a short-lived intermediate product when no-carrier-added (n.c.a.) products are sought.

The first reaction $W-186(n,\gamma)W-187$ proceeds relatively efficiently due to a significant thermal cross-section of $\sigma_{th} = 38.1(5)$ b plus a considerable contribution of resonance capture of epithermal neutrons, see Figure 2. Here the pink line with evaluated/recommended cross-sections is based on actually measured neutron resonances.

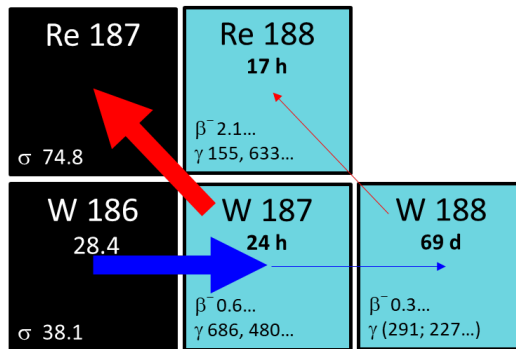


Figure 1: Reaction path relevant for the production of W-188 in a high thermal neutron flux.

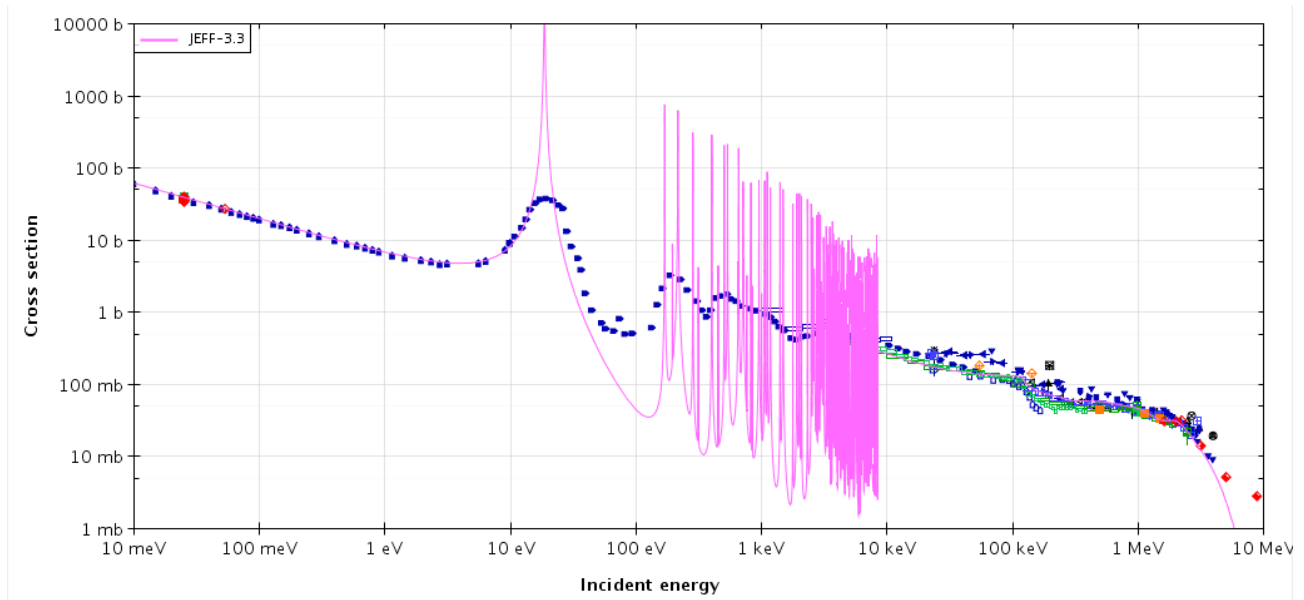


Figure 2: Experimental (points) and evaluated (pink line) $W-186(n,\gamma)W-187$ cross-section as function of neutron energy.

The cross-section of the second step $W-187(n,\gamma)W-188$ is less well known. W-187 is too short-lived and thus not suitable as target for direct energy-dependent cross-section measurements. The thermal cross-section can be derived indirectly from measured yields of W-188 produced in two subsequent captures. An earlier work gave a value of $\sigma_{th} = 64(10)$ b [J.H. Gillette, 1966. Review of Radioisotope Program, 1965, Report ORNL-4013, Oak Ridge National Laboratory], while more recently a tenfold smaller number of $\sigma_{th} = 6.5(8)$ b has been reported [O.A. Ersöz et

al., Appl Radiat Isot 2019;148:191.]. The latter is more in line with the experimentally observed W-188 yields. Figure 3 shows also a possible energy dependence of the W-187(n, γ) cross-section, but this is purely theoretical, based on the TALYS statistical model.

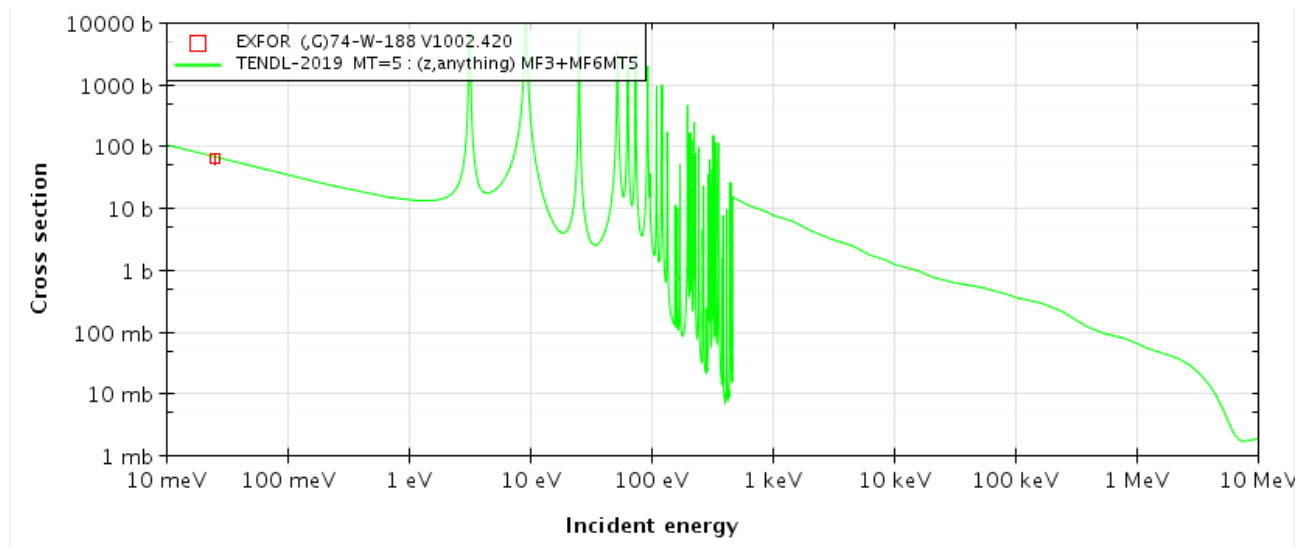


Figure 3: Experimental (red point) and theoretical (green line) W-187(n, γ)W-188 cross-section as function of neutron energy.

Considering a capture cross-section of $\sigma_{\text{th}} = 6.5 \text{ b}$ and a thermal neutron flux of $\Phi = 10^{15} \text{ cm}^{-2}\text{s}^{-1}$, it would take 2.4 years to transmute half of a certain amount of W-187 atoms to W-188. In reality W-187 is radioactive and decays with a half-life of 1 day, i.e. most of it will decay to Re-187 instead of capturing a neutron and only a tiny fraction of 0.08% of W-187 proceeds via the second step to W-188. This situation is highlighted in Figure 1 by the relative thickness of the arrows. Contributions of epithermal neutron capture can slightly improve the fraction that undergoes capture to W-188, but overall the fundamental challenge for large-scale production of W-188 (and hence for large-scale application of W-188/Re-188 generators) is directly linked to these unfavourable cross-sections.

Let's now consider a twice higher neutron flux of $\Phi = 2 \cdot 10^{15} \text{ cm}^{-2}\text{s}^{-1}$. This would double the capture rate of the first step W-186(n, γ)W-187, producing twice more W-187. However, it would also double the capture rate of the second step W-187(n, γ)W-188, i.e. double the chance that a W-187 captures a neutron before decaying. Overall the W-188 yield would be increased by the product of both factors, i.e. two times two equals fourfold. Obviously, a twice lower neutron flux would be fourfold penalizing in terms of W-188 yield reduction.

Hence, **in double neutron capture reactions the yield of the final product scales proportionally to the square of the neutron flux Φ** (at equal irradiation time). We note that this applies for the *yield*, i.e. the produced W-188 activity per gram of W-186 starting material. In turn the *specific activity*, i.e. the produced W-188 activity per gram of tungsten remaining after the irradiation is slightly higher than the yield because the part of tungsten meanwhile transmuted to rhenium or osmium does not count here.

Since the W-188 yield is inherently low one has to increase the W-186 target mass to produce the required W-188 activities. However, a significant increase of target mass can have a negative feedback on the neutron flux in the target and thus on the yield. Let us consider a very thick target: neutrons that have already been absorbed in an outer layer of the target are no longer available to penetrate deeper into the target, i.e. the neutron flux will diminish inside the target. This so-called *neutron self-shielding* of targets can be described analytically for simple geometries such as spheres, cylinders or foils when only thermal neutrons are considered.

Alternatively, one can perform Monte Carlo simulations that accounts for the neutron self-shielding as function of neutron energy, i.e. also for epithermal neutrons, as well as for changes of the neutron spectrum induced by absorption, scattering or moderation in the sample and its environment.

Actual targets are rarely exactly spherical, but we first demonstrate the effect of neutron self-shielding at hand of spherical samples using the empirical formulae given by E. Martinho et al. [J Radioanal Nucl Chem 2004;261:637.].

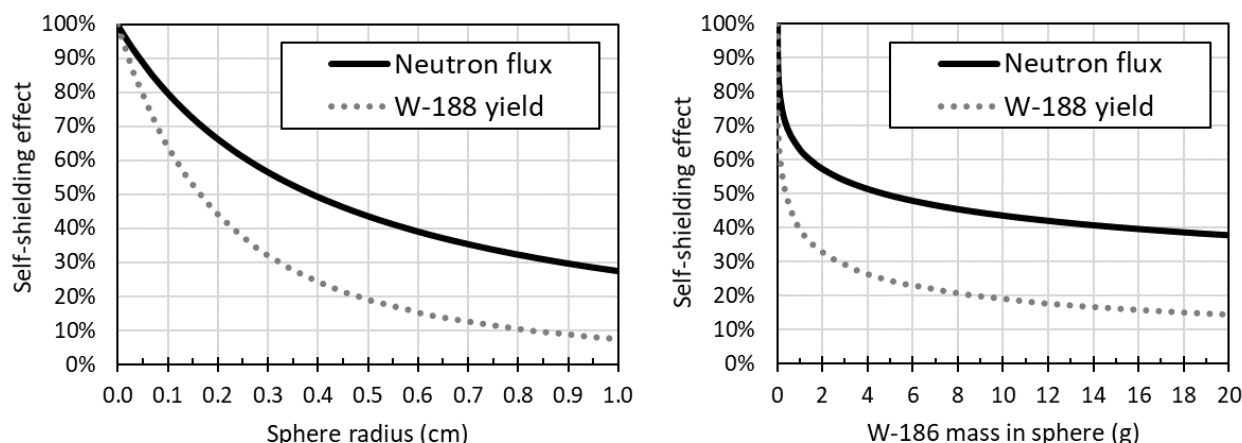


Figure 4: Analytically estimated neutron self-shielding in spherical W-186 targets (density 19.3 g/cm³) as function of sphere radius (left) or sphere mass (right) respectively. The W-188 yield scales with the square of the neutron flux.

Figure 4 shows the result of this analytical estimate of neutron self-shielding. Already at a sphere radius of 0.39 cm, corresponding to a W-186 mass of 4.8 g, the average neutron flux in a dense sphere of metallic W-186 drops to 50% of the unperturbed neutron flux. Consequently, the W-188 yield drops to only 25% of the unperturbed value. Much smaller radii and masses are required if one wants to maintain the W-188 yield at a higher level, e.g. a 0.05 cm sphere radius, corresponding to a W-186 mass of only 10 mg, would keep the W-188 yield at 79% of the unperturbed value. Either of these solutions is unfavorable for actual production purposes, in the first case (≈ 5 g sphere) the specific activity could drop below the minimum useful for generator loading, in the second case (10 mg sphere) the overall mass and activity would be too low.

This issue of strong neutron self-shielding stems from the high density of metallic tungsten combined with its significant absorption cross-section. The density of 19.3 g/cm³ corresponds to a number density of $6.3 \cdot 10^{22}$ cm⁻³ and consequently a macroscopic cross-section (the product of microscopic cross-section and number density) of 2.4 cm⁻¹ and a mean free path (the inverse of the macroscopic cross-section) of only 0.42 cm.

Since we cannot change the microscopic cross-section, the only potential variable is the number density. Let us imagine we could reduce the number density freely by “adding empty space” between the strongly absorbing W-186 atoms. Again, we can model this situation analytically considering a sphere of fixed radius, say 1.704 cm, that would correspond to 400 g of dense metal mass. However, now we change the number density between 0% and 100% of dense metallic tungsten. Figure 5 shows the result.

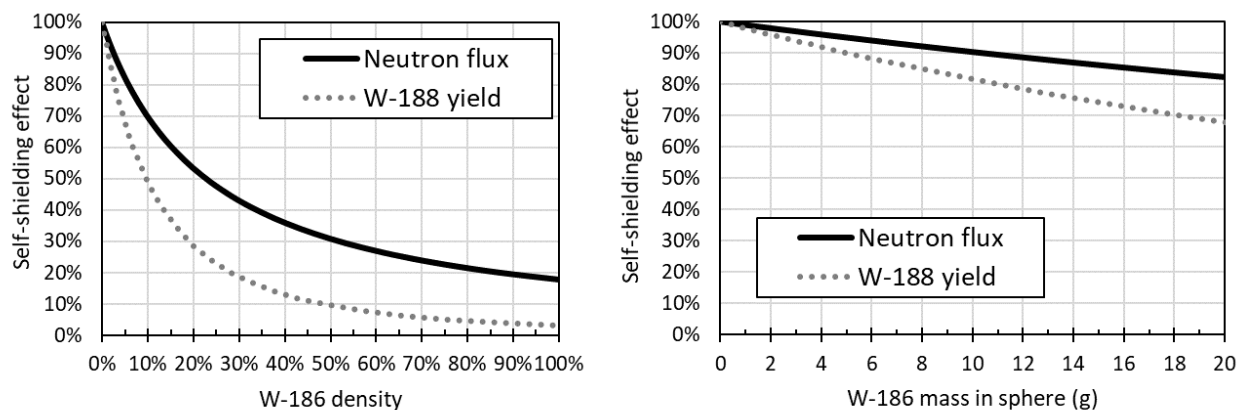


Figure 5: Analytically estimated neutron self-shielding in spherical W-186 targets (1.704 cm radius) as function of number density, relative to dense metallic tungsten (left) or mass contained in such a low-density target (right), respectively.

Figure 5 shows that a reduction of density is beneficial for the neutron flux and the W-188 yield. Filling a sphere of 1.704 cm radius with 5% of metallic tungsten density, i.e. with 20 g of W-186 in the sphere, maintains the neutron flux at 82% of the unperturbed value and the W-188 yield at 68%. Reducing the density further to 2.5% of metallic tungsten density, i.e. with 10 g of W-186 in the sphere, maintains the neutron flux above 90% of the unperturbed value and the W-188 yield at 82%. Thus, such a geometry is far more promising for actual production than the previously considered dense metal sphere. Now one could load with double the mass (10 g versus 4.8 g discussed above) but the W-188 yield remains at 82%, versus 25% previously, a factor 3.3 gain in yield (and nearly as much in specific activity)!

This gain arises because a larger sphere has a larger surface, i.e. with a fixed neutron flux Φ (in $\text{cm}^{-2}\text{s}^{-1}$) incident on a larger sphere in total more neutrons traverse the sphere's surface. If the same number of W-186 atoms present in a larger sphere absorbs a certain number of neutrons, this number of lost neutrons represents a smaller fraction of all incident neutrons and the self-shielding effect is correspondingly less pronounced.

Let us now consider an inhomogeneous distribution of a fixed amount of W-186 in the sphere. One extreme case had been considered above already: a dense sphere in the centre. The opposite extreme would be a hollow sphere with a thin shell of 100% density. This geometry is not readily described by the analytical formulae given by E. Martinho et al., but it can be easily calculated with a Monte Carlo model.

To obtain a situation closer to reality the modelling considered the W-186 samples placed without further enclosure into the V4 beam tube that is embedded in a full model of the RHF reactor [OCDE-NEA. Evaluation of measurements performed on the French high flux reactor (RHF), Rev. 2, October 2011. NEA/NSC/DOC(2006)1 RHF-FUND-RESR-00]. The modelling was performed by MCNP version 6.2.0 [J. Werner, et al. "MCNP User's Manual Code Version 6.2. Los Alamos National Laboratory" - Tech. Rep. LA-UR-17-29981 (2017)] chosen for future compatibility in the frame of HEU/LEU conversion. Cross-sections were imported from JEFF3.3 [J. Werner, et al. "MCNP User's Manual Code Version 6.2. Los Alamos National Laboratory" - Tech. Rep. LA-UR-17-29981 (2017)]. This modelling accounts in detail for the modification of the unperturbed neutron flux by the presence of the samples and their environment via absorption, scattering or moderation respectively. Consequently, the perturbed self-shielded neutron flux and realistic capture rates are obtained.

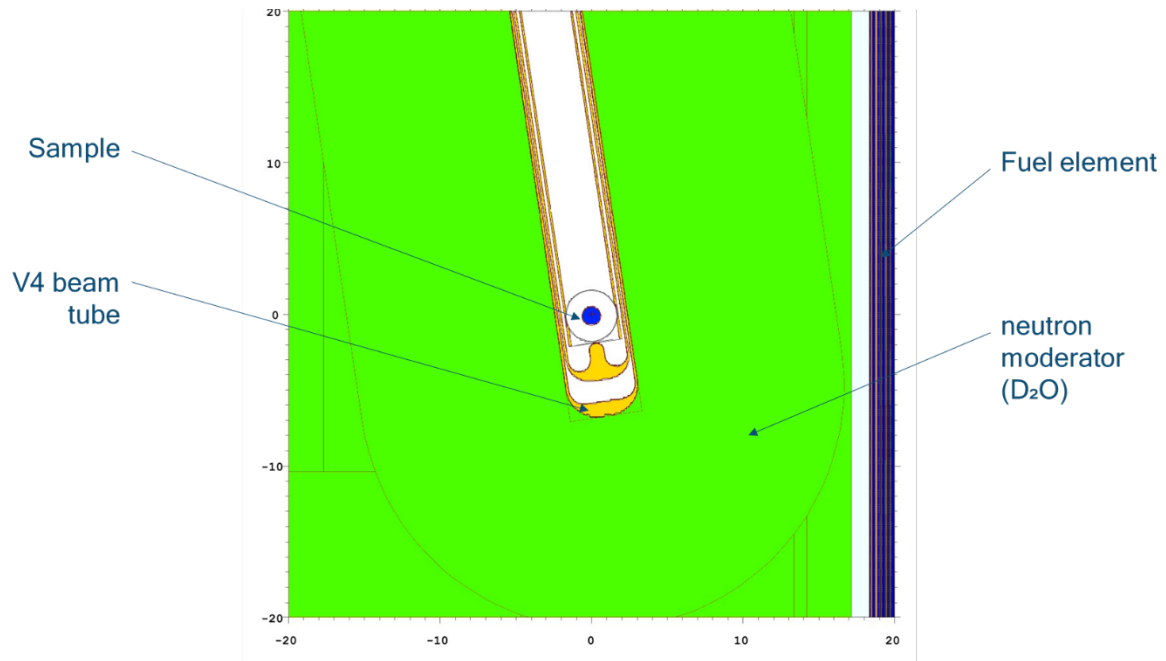


Figure 6: MCNP model of a spherical sample placed in the V4 beam tube of the RHF reactor at ILL. Heavy water in green, aluminium in yellow, W-186 in blue.

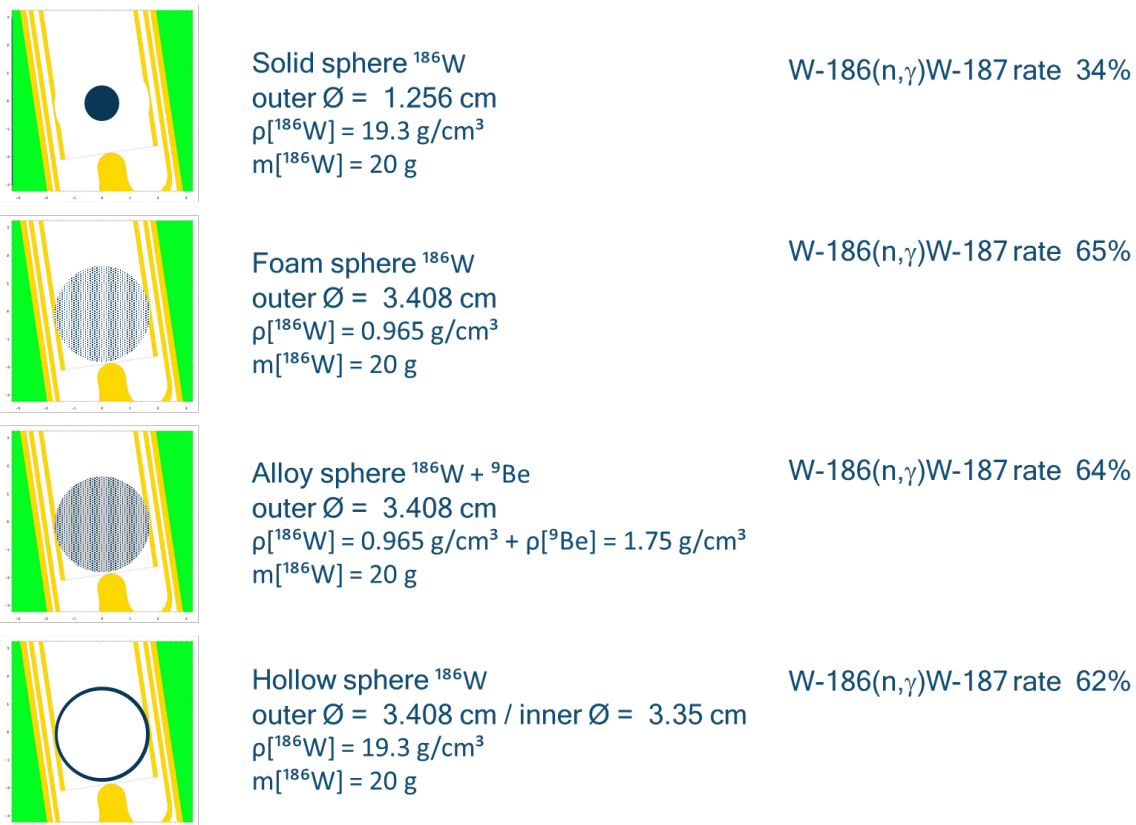


Figure 7: Four sample configurations simulated with the MCNP model. The self-shielded W-186(n, γ)W-187 capture rates (atoms W-187 produced per gram W-186 and second) are given with respect to the capture rates in an empty sphere, i.e. without self-shielding. These capture rates are proportional to the self-shielded perturbed neutron flux.

We observe that the MCNP calculation gives a somewhat higher self-shielding correction than the analytical calculation, e.g. 34% for the compact 20 g sphere compared to 38% for the analytical calculation (see Figure 4, right side). Indeed the MCNP calculation accounts also for the supplementary production by epithermal neutrons while the analytical calculation

considers thermal neutrons only. As shown on Figure 2 the epithermal region is characterized by individual very strong resonances. The peak cross-sections of such resonances can be much higher than the thermal neutron cross-section. Consequently, the mean free path of neutrons that happen to have the suitable energy of such a resonance is much shorter and the self-shielding effect is more pronounced. We retain that the analytical estimate gives a good guidance of the magnitude of self-shielding while a more precise analysis is possible with a Monte Carlo simulation. However, even the best simulation will not be able to make up for theoretical uncertainties such as the experimentally unknown resonances of the second reaction step $W-187(n,\gamma)W-188$. Depending if these resonances (for predictions see Figure 3) are located at the same energies as those of $W-186(n,\gamma)$ (see Figure 2) or not, the self-shielding caused by $W-186$ will or will not affect the epithermal neutron capture of $W-187$. Thus, the $W-188$ yield might not necessarily scale exactly with the square of the neutron flux once the contribution by epithermal neutron capture is considered.

So far we had discussed a theoretical, perfectly spherical geometry. In practice, the geometry would be rather cylindrical. Samples to be irradiated in the V4 beam tube of ILL's high flux reactor RHF or in the beam tubes of SCK's high flux reactor BR2 are usually encapsulated into aluminum capsules with 2 cm inner diameter and <6 cm usable height. Thus, the sample could cover a cylindrical space of about 16 to 18 cm³ or somewhat less when it is enclosed in a separate sample containment, e.g. a large quartz ampoule.

We will consider a cylindrical geometry with 2 cm diameter and 5 cm height and apply the analytical formula for cylinder geometry given by E. Martinho et al. [J Radioanal Nucl Chem 2004;261:637].

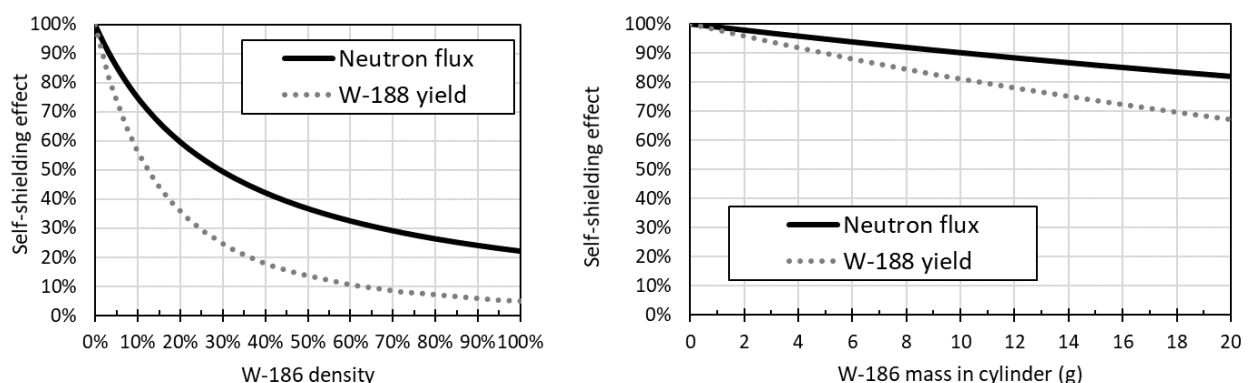


Figure 8: Analytically estimated neutron self-shielding in cylindrical W-186 targets (1 cm radius, 5 cm height) as function of number density, relative to dense metallic tungsten (left) or mass contained in such a low-density target (right), respectively.

Filling a cylinder of 1 cm radius and 5 cm height with 6.6% of metallic tungsten density, i.e. with 20 g of W-186 in the cylinder, maintains the neutron flux at 82% of the unperturbed value and the W-188 yield at 67%. Considering that the true self-shielding accounting for all effects beyond the analytical description will be slightly worse, such a number appears as a suitable compromise between produced activity and achieved yield or specific activity respectively and will be considered as objective for real geometries to be discussed in the following section. In practise, it might be required to reduce the W-186 mass somewhat, but even a mass of say 10 g per irradiation capsule would be a major gain with respect to prior irradiations of oxide targets where the W-186 mass per irradiation capsule was only ≈ 3 g, see Figure 3 of deliverable D3.1.

3 POSSIBLE GEOMETRIES OF ADVANCED TUNGSTEN TARGETS

3.1 Theoretical Geometries

As discussed above, different geometrical realisations would lead to similar neutron self-shielding, provided a similar W-186 mass is distributed over an area circumscribed by a similar external volume. In particular, the microstructure of a sample plays no role for the neutronics properties, provided the linear dimensions are small with respect to the mean free path, here 0.42 cm in dense tungsten. This enables a multitude of practical realisations. Some examples are shown in Figure 9.

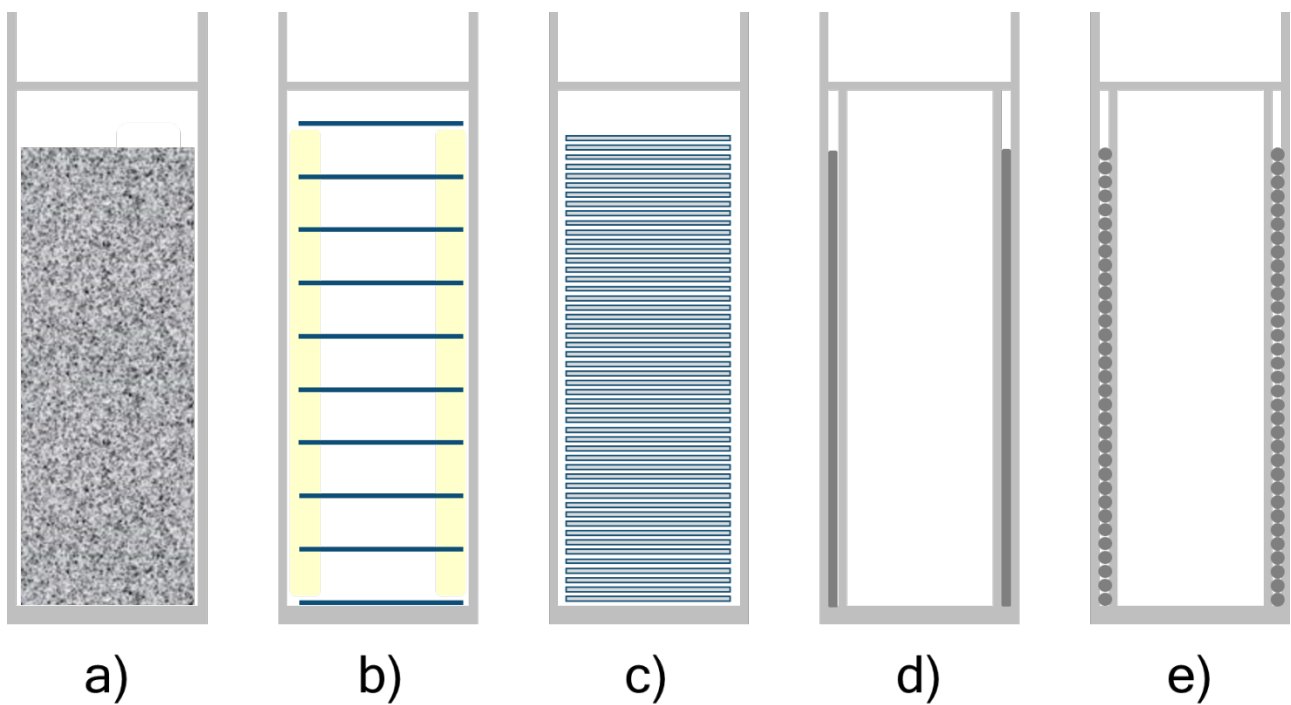


Figure 9: Schematic representation of different geometries of advanced W-186 targets that would all fill or circumscribe roughly a cylinder with 1 cm radius and 5 cm height.

- a) A low-density “foam-like structure” with high porosity or an alloy with a weakly neutron absorbing material.
- b) A “wedding-cake” structure where disks of W-186 are held apart with spacers of weakly neutron absorbing material.
- c) A “pancake tower” structure where disks of weakly neutron absorbing material are coated with thin layers of W-186.
- d) A “hollow cylinder” where the space between two concentric cylinders made from weakly neutron absorbing material is filled with W-186.
- e) A “wire coil” where a W-186 wire (or mesh or foil or similar structures) is wrapped around an inner cylinder made from weakly neutron absorbing material.

Since several of the presented geometries rely on some additional “weakly neutron absorbing material” it is useful to recall examples of such materials.

3.2 Filler materials

Table 1 provides a summary of the characteristics relevant for neutronics calculations with weakly neutron absorbing materials as well as W-186 in metallic or oxide form. The (molar) microscopic scattering cross-section σ_s and absorption cross-section σ_a are multiplied with the number density to yield the macroscopic absorption cross-section Σ_a or total macroscopic cross-section Σ_t respectively. The inverse of the latter provides the mean free path of the neutrons before undergoing any interaction (scattering or absorption). The last column shows the neutron self-attenuation analytically calculated for a dense cylinder with 1 cm radius and 5 cm height, cf. left side of Figure 8 for metallic W-186.

Table 1: Neutronics characteristics of weakly neutron absorbing materials compared to W-186 in metallic or WO₃ form.

Material	ρ g/cm ³	Number density at./cm ³	σ_s b	σ_a b	Σ_a cm ⁻¹	Σ_t cm ⁻¹	λ_t cm	Φ/Φ_0
W-186	19.3	6.2E+22	0.065	38.1	2.4	2.4	0.42	0.22
[W-186]O ₃	7.16	1.8E+22	12.8	38.1	0.70	0.94	1.1	0.49
Be	1.85	1.2E+23	7.63	0.0076	0.0009	0.95	1.1	1.00
C	1.54	7.7E+22	5.55	0.0035	0.0003	0.43	2.3	1.00
Al	2.7	6.0E+22	1.50	0.23	0.014	0.10	9.6	0.97
Si	2.33	5.0E+22	2.17	0.17	0.0085	0.12	8.6	0.98
Al ₂ O ₃	3.98	2.3E+22	15.7	0.46	0.011	0.38	2.6	0.97
SiO ₂	2.2	2.2E+22	10.6	0.17	0.0038	0.24	4.2	0.99

We can observe that due to the lower number density of WO₃, the latter shows significantly less neutron self-shielding compared to metallic W. Here the oxygen atoms act microscopically as a kind of “filler material” that pushes the W atoms further apart.

All other materials in Table 1 do have significant scattering cross-sections, but small or very small absorption cross-sections. While the mean free path λ_t for any interaction is only few cm, most interactions result just in scattering where the neutron may change its direction but is not absorbed. Consequently, the neutron flux is barely reduced as can be seen in the last column. Thus, such “weakly neutron absorbing materials” could well be used as filler materials to realize some of the geometries shown in Figure 9.

The case of a solid alloy of 5% W-186 and 95% Be has also been included in the MCNP simulation, see second line of Figure 7. Within the precision of the calculation the resulting neutron self-shielding factor of 64% is identical to that of a W-186 foam with 5% density but no added Be, namely 65% self-shielding. The Monte Carlo calculation thus confirms that a mixture with weakly neutron-absorbing materials to “dilute” the W-186 is an efficient strategy to reduce the neutron self-shielding.

4 PRACTICAL REALISATION

4.1 Foam-like structure or alloy

Low density metal foams, also called metal sponge, can be generated by a replica method based on a skeleton made from polymers or by injecting gas bubbles or a foaming agent into molten metal. The latter method is more challenging for tungsten than for other metals due to its high melting point and high buoyancy that drives out the gas bubbles.

Alternatively the metal layer can be deposited by chemical vapour deposition on a high temperature stable skeleton such as reticulated vitreous carbon (RVC). As seen from Table 1, pure RVC would be suited as weakly neutron-absorbing matrix.

Tungsten foam, tungsten sponge or tungsten coated RVC can be found on the websites of commercial suppliers [<https://ultramet.com/> or <https://www.americanelements.com/tungsten-foam-7440-33-7>], but the former did not reply to requests and the latter declared that tungsten foam is presently not available.

Complex hollow structures can be generated by selective laser sintering (SLS, also known as 3D-laser printing) of tungsten powder. A test piece produced at EOS Finland has been obtained and will be used for chemical dissolution tests and analysis. However, this method requires usually more starting material to fill the entire powder bed of the SLS machine, clearly a challenge when expensive enriched starting materials are required.

Also felt-type materials consisting of interleaved micro- or nanoscopic metal fibres can be considered, provided they are mechanically sufficiently stable for handling, e.g. to fill target containers in a controlled way, and thermally and mechanically robust to keep their integrity during and after the irradiation. A test sample of tungsten fibre felt has been obtained from Fermilab (US). It had been produced by electrospinning, then annealed at 850 °C in nitrogen to convert the metalorganic precursor to a purely inorganic compound [cf. V. Kundrat et al., Int J Refract Met H 2023;112:106121].

Alternatively to open or closed pores that are gas-filled one can reduce the average tungsten density also by alloying or mixing with a weakly neutron-absorbing material. A Be-W mixture had been selected for the MCNP calculation, but in practise other elements can be handled more easily than beryllium. For example aluminium could be used. It can either serve as true alloying element, e.g. as Al₁₂W alloy or still higher aluminium content, or as a solid-state matrix into which tungsten powder or tungsten grains are incorporated, e.g. by cold rolling, similar to the preparation of dispersion fuel for research reactors. However, one important challenge when using aluminium as filler material will be the management of this aluminium during dissolution of the irradiated targets and when loading the W-188/Re-188 generators. Test samples with large aluminium excess have been prepared (see 4.3 below) that will allow studying these issues.

4.2 Wedding-cake structure

Thin disks of sintered tungsten powder can be prepared by selective laser sintering (SLS, see above) or by spark plasma sintering (SPS). For the latter method, tungsten powder is enclosed between graphite dies through which DC or AC current is passed. Due to the geometric constraint by the dies far less powder is required compared to SLS. However, it needs to be investigated if surface layers of tungsten carbide are formed that could disturb the dissolution process. Test samples prepared by SPS at CEA Grenoble with tungsten powder of different granulometry were obtained and will be used for chemical investigations of the dissolution behaviour.

4.3 Pancake tower structure

In practice, the minimum thickness of samples prepared by SLS or SPS is limited by the mechanical stability of the disks. If the tungsten thickness should be reduced even further a support matrix will be required. The tungsten coating can be realized either by chemical vapor deposition (CVD) or by physical vapor deposition (PVD). We explored the latter, namely DC magnetron sputtering performed at ILL to produce test samples. Different supports have been studied, namely silicon wafers (0.3 mm thickness), sapphire plates (0.2 mm thickness), high purity (99.99+%) aluminum foil (0.025 mm thickness), Al5754 alloy foil (0.2 mm thickness) and borosilicate glass (1 mm thickness). The latter serves only for deposition/dissolution studies, but cannot be used for irradiations due to excessive neutron absorption by the boron content. Tungsten deposits of 1 μm , 2 μm and 4 μm thickness have been realized. However, for some backings the strain of the deposited layer was significant, thus the thickest layers could not be realized for all backing types. A dedicated single crystal silicon substrate placed next to the other samples was used to estimate the residual stress inside the 1 μm coating by the curvature method. It gave a result of ≈ 2.5 GPa in compression. Dissolution tests with the samples will show if the sputtering process has introduced any other metallic impurities.

4.4 Hollow cylinder

A hollow cylinder structure can be easily realized, e.g. by two concentric cylinders made from metal, e.g. aluminium, or from non-metals, e.g. quartz. In the simplest realization, one could fill the intermediate space with tungsten powder. However, for the handling after the irradiation it is preferable to fill the intermediate space with more mechanically stable forms, e.g. with tungsten felt (cf. 4.1).

4.5 Wire coil

A wire coil or a foil or mesh wrapped around an inner cylinder would provide a geometry similar to point 4.4, probably with better mechanical stability. However, to produce enriched W-186 targets in this way the W-186 would need to be made available in form of wires, mesh or foil. It remains a challenge to perform this efficiently with a small quantity of enriched W-186.

However, the foil geometry allows for an easy check how the partial transmutation of W to Re during a long irradiation would affect the dissolution behaviour. Test samples of identical geometry, but with different stoichiometry ($\text{W}_{0.97}\text{Re}_{0.03}$ and $\text{W}_{0.75}\text{Re}_{0.25}$) have been obtained from Goodfellow, UK for this purpose.

5 CONCLUSIONS AND OUTLOOK

Different geometries of low-density or hollow targets made from metallic enriched W-186 have been considered theoretically in terms of neutronics properties. Practical realisations of certain geometries are discussed and test pieces prepared with different methods have been sent to the SECURE partner NCBJ for dissolution studies and chemical analysis. Results from these studies will allow classifying the most promising materials that could then be tested as advanced metal targets to secure and improve the production of W-188.

6 ACKNOWLEDGEMENTS

The exploration of a large diversity of different types of tungsten metal targets goes far beyond the technological capabilities of a single lab. We are very grateful for the excellent collaboration with and contributions by colleagues from many different labs: Thierry Bigault and Guillaume Delphin (ILL Grenoble) for test pieces prepared by sputter deposition, Matthieu Boidot (CEA Grenoble) for test pieces prepared by spark plasma sintering, Silvia Candela (INFN Padova), Mattia Manzolaro (INFN Padova), Pietro Rebesan (INFN Padova) and Elina Väihkönen (EOS Finland) for test pieces prepared by selective laser sintering and Sujit Bidhar (FNAL Batavia) and Kavin Ammigan (FNAL Batavia) for test pieces prepared by electrospinning,